Journal of Fluorine Chemistry 137 (2012) 27–33

Contents lists available at SciVerse ScienceDirect

Journal of Fluorine Chemistry

journal homepage: www.elsevier.com/locate/fluor

NIR-labeled perfluoropolyether nanoemulsions for drug delivery and imaging

Claire E. O'Hanlon [a], Konjit G. Amede [a], Meredith R. O'Hear [b], Jelena M. Janjic [a,*]

[a] Graduate School of Pharmaceutical Sciences, Duquesne University, Pittsburgh, PA 15282, United States
[b] Department of Biological Sciences, Carnegie Mellon University, Pittsburgh, PA 15213, United States

ARTICLE INFO

Article history:
Received 18 August 2011
Received in revised form 3 February 2012
Accepted 7 February 2012
Available online 15 February 2012

Keywords:
Theranostic
PFPE
NIR
Drug delivery
Imaging
^{19}F MRI

ABSTRACT

Theranostic nanoparticle development recently took center stage in the field of drug delivery nanoreagent design. Theranostic nanoparticles combine therapeutic delivery systems (liposomes, micelles, nanoemulsions, *etc.*) with imaging reagents (MRI, optical, PET, CT). This combination allows for non-invasive *in vivo* monitoring of therapeutic nanoparticles in diseased organs and tissues. Here, we report a novel perfluoropolyether (PFPE) nanoemulsion with a water-insoluble lipophilic drug. The formulation enables non-invasive monitoring of nanoemulsion biodistribution using two imaging modalities, ^{19}F MRI and near-infrared (NIR) optical imaging. The nanoemulsion is composed of PFPE-tyramide as a ^{19}F MRI tracer, hydrocarbon oil, surfactants, and a NIR dye. Preparation utilizes a combination of self-assembly and high energy emulsification methods, resulting in droplets with average diameter 180 nm and low polydispersity index (PDI less than 0.2). A model nonsteroidal anti-inflammatory drug (NSAID), celecoxib, was incorporated into the formulation at 0.2 mg/mL. The reported nanoemulsion's properties, including small particle size, visibility under ^{19}F NMR and NIR fluorescence spectroscopy, and the ability to carry drugs make it an attractive potential theranostic agent for cancer imaging and treatment.

1. Introduction

Many anticancer agents, from hormonal modulators to anti-proliferative agents, suffer from low selectivity, high toxicity and low water solubility. Numerous nanoparticles, liposomes, micro-emulsions, and nanoemulsions have been formulated to increase drug solubility, improve drug accumulation at the site of action, and avoid the side effects of systemic exposure [1]. However, major challenges in cancer nanotherapeutics remain; among these are determining if the drug formulation reaches the desired site of action, how long it remains there, and the time it takes for the formulation to be eliminated from both the site of action and the body. Accurately answering these types of questions would greatly improve therapeutic nanoparticle dosing and patient safety. Introducing an imaging agent to drug delivery nanoparticles is a critical component in answering these questions. Fortunately, many groups are currently exploring theranostic approaches. In one recent report, a "theranostic" platform was based on oil-in-water nanoemulsions with incorporated iron oxide (IO) nanocrystals for magnetic resonance imaging (MRI), the fluorescent dye Cy7 for near-infrared (NIR) fluorescent imaging, and the hydrophobic glucocorticoid prednisolone acetate valerate (PAV) for therapeutic purposes [2]. This was an encouraging precedent to our study demonstrating the usefulness of combining MRI with a NIR imaging modality. Other examples of MRI detectable drug loaded nanoparticles have been recently reviewed [3]. However, our goal was to introduce a ^{19}F MRI modality that can provide quantitative assessment of the theranostic distribution in tissue [22]. This presents as a clear advantage over IO based MR contrast agents. Contributing to the improved understanding of cancer nanotherapeutic behavior, we report the design, development and *in vitro* biological testing of a novel ^{19}F MR and NIR fluorescent perfluorocarbon-based nanoemulsion for parenteral delivery of water-insoluble drugs. The PFPE nanoemulsion reported here incorporates dual imaging modalities, designed to allow specific and selective biodistribution assessment *in vitro* and *in vivo*. Each imaging modality complements the other. The key advantages for using ^{19}F for *in vivo* imaging of therapeutic nanoparticle accumulation are: (1) MR images have superior selectivity for ^{19}F in therapeutic nanoparticles, with no background signal; (2) the detected ^{19}F signal is independent of individual tissue variability or physiological status; (3) ^{19}F MR signal can be used to quantify the organic ^{19}F present in the body upon administration of the nanoemulsion while conventional ^{1}H anatomical images can be used to place drug delivery particles into their anatomical context [4]. ^{19}F has low biological abundance and there is no

* Corresponding author at: 401 Mellon Hall, Graduate School of Pharmaceutical Sciences, Duquesne University, 600 Forbes Avenue, Pittsburgh, PA 15282, United States. Tel.: +1 412 396 6369.
E-mail address: janjicj@duq.edu (J.M. Janjic).

0022-1139/$ – see front matter © 2012 Elsevier B.V. All rights reserved.
doi:10.1016/j.jfluchem.2012.02.004

organic ^{19}F in the body, which makes ^{19}F MR detection highly selective for the nanoemulsion introduced. However, the gyromagnetic ratios of ^{1}H and ^{19}F differ by about 6% and the relative sensitivity is 0.83, which requires a high field magnet for sufficient detection at low concentrations [4]. Consideration must be given to the choice of in-plane resolution and slice thickness to maximize the ^{19}F voxel concentration while satisfying the desired anatomical localization [5]. Recent studies successfully used perfluorocarbon (PFC) nanoreagents to track inflammatory cell accumulation in transplantation and experimental autoimmune encephalomyelitis (brain inflammation) models with high selectivity and sensitivity [5,6]. Additionally, PFC nanoreagents have recently been used to deliver therapeutic peptides [7]. Perfluoropolyethers (PFPEs) have been used extensively by our group and others formulated into biocompatible nanoemulsions for therapeutic cell tracking by ^{19}F MRI *in vivo*. PFPEs are highly chemically stable and biologically inert polymers with high content of MR equivalent ^{19}F nuclei per molecule providing high sensitivity for the *in vivo* imaging. PFC molecules such as perfluorooctylbromide (PFOB) and perfluoro-15-crown-5 ether (PCE) have been formulated into emulsions and nanoemulsions for blood substitute development since the late 1980s. However, there are limited reports on the long term stability of these formulations. Ostwald ripening is a major degradation mechanism in nanoemulsions. It has been demonstrated that the structure and molecular size of the oil phase has dramatic impact on the rate of the ripening [8]. Most small molecule PFC formulations reported are typically destabilized by Ostwald ripening, which is known to decrease as molecular weight of the PFC increases [4]. PFPEs are long PFC chains of (CF_2CF_2O) monomers, which have exceptionally low water solubility, likely contributing to the exceptionally high stability of PFPE nanoemulsions without increasing droplet size and polydispersity [4,21]. PFPE nanoemulsions provide sustained droplet size over times which is critical for future clinical applications as drug delivery vehicles.

The second imaging modality, NIR fluorescent imaging, overcomes potential issues in biodistribution studies using ^{19}F detection *in vivo*, such as lack of access to a high magnet, cost, and potentially insufficient sensitivity. NIR dyes are used for various applications in intracellular imaging and post-imaging histological analysis. Compared to many alternatives, *in vivo* NIR fluorescence imaging is safe, fast, inexpensive, and relatively easy to use. In subcutaneous tumor models, commonly used in preclinical testing of nanoparticle drug delivery and targeting, NIR imaging has sufficient tissue penetration depth (up to several millimeters in a reflectance configuration and 30–40 cm in a tomographic configuration) for imaging in most preclinical models [9] and can complement the ^{19}F MRI assessment. PFC nanoemulsions incorporating NIR fluorescence imaging probes have been previously used to label dendritic cells *in vitro* and *in vivo* [10]. Doxorubicin, a fluorescently active chemotherapeutic agent, was previously encapsulated in PFC nanodroplets and used for NIR biodistribution studies of ultrasound-mediated drug delivery [11]. However, these formulations produced multimodal particle size distributions with at least one mode above 300 nm. In the current study, the perfluorocarbon/NIR reagent has been designed to have unimodal particle size distribution with average size less than 200 nm and with the additional imaging modality of ^{19}F MRI.

Nanoemulsions have emerged as an attractive drug delivery vehicle for water-insoluble drugs. The diameter of the nanoemulsion droplets should be less than 200 nm to take advantage of passive targeting by the enhanced permeability and retention (EPR) effect in tumors and sites of inflammation [12,13]. Nanoemulsions of this size would also be suitable for parenteral administration of water-insoluble drugs [14]. Additionally, the nanoemulsion's PDI must be sufficiently low (<0.2) to maintain the vehicle's effectiveness, as a high PDI indicates multimodal (or a very wide unimodal) particle size distribution. With these characteristics, nanoemulsions have great potential for improving cancer treatment, particularly in passive targeting of tumor-induced inflammation. Infiltration of primary tumors with inflammation-promoting cells has been proposed to be a promoter of tumor growth and chronic inflammation [15]. Cyclooxygenase-2 (COX-2)-derived bioactive lipids, including prostaglandin E2, are potent inflammatory mediators that promote tumor growth and metastasis [16]. Recent epidemiological studies demonstrated that treatment with non-steroidal anti-inflammatory agents (NSAIDs), such as COX-2 inhibitors, can reduce the risk of developing breast cancer; aspirin and celecoxib show the most significant effects [17,18]. Celecoxib, a selective COX-2 inhibitor, has been recently recognized as a potential cancer adjuvant therapeutic agent. It was used here as a model water-insoluble drug.

In the present study, nanoemulsions containing PFPE-tyramide, nonionic surfactants, and a hydrocarbon oil were prepared and characterized. Microfluidization techniques yielded a stable formulation for a nanoemulsion with NIR dye and celecoxib. The formulation was evaluated *in vitro* in a model immune cell line, fetal skin dendritic cells (FSDCs), for cellular uptake and toxicity. Cellular loading of the drug carrying nanoemulsion was evaluated by NIR microscopy, NIR spectroscopy and quantified by ^{19}F NMR.

2. Results and discussion

2.1. Composition and structure of PFPE-tyramide nanoemulsions

Several characteristics of PFPEs make them useful as MRI agents and drug delivery vehicles. The carbon-fluorine bond is highly chemically stable; there are no known enzymes that degrade PFCs *in vivo* [4]. PFPEs have no apparent biological reactivity or cell toxicity. An advantageous property of perfluorocarbons is the "fluorophobic effect," wherein they tend to assemble into their own phase that is neither hydrophilic nor lipophilic [19]. This property can be exploited to produce a variety of fluorocarbon-based emulsions using both self-assembly and high shear methods in the presence of hydrocarbon oils, lipids and nonionic surfactants [4]. Here we report a unique PFPE conjugate which can form nanoemulsions in the presence of hydrocarbon oils and nonionic surfactants. Initially, we chose to conjugate tyramine **2** to the reactive ends of the PFPE dimethyl ester polymer **1** for two reasons: (1) fluorocarbon–hydrocarbon conjugates are known to self-assemble [20], and (2) it would be relatively easy to conjugate other moieties to the phenol on tyramine in the future. PFPE-tyramide **3** was synthesized and purified using our earlier reported protocol [21], Scheme 1, with some modifications. Briefly, PFPE dimethyl ester **1** is reacted with tyramine **2** in trifluoroethanol at

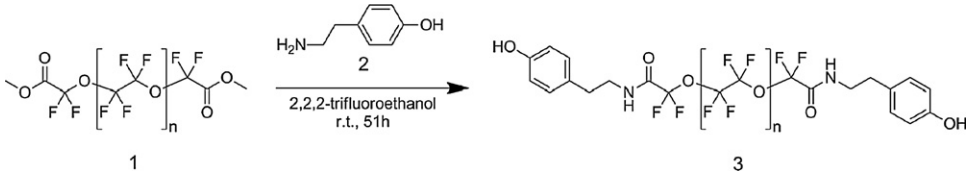

Scheme 1. Synthesis of PFPE-tyramide.

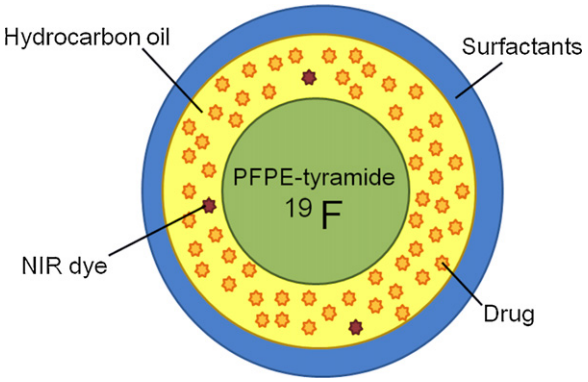

Fig. 1. Proposed schematic of a PFPE-tyramide nanoparticle.

room temperature under inert atmosphere; after 2 days solvent is removed under vacuum, and product purified on silica gel to obtain PFPE-tyramide **3** as a waxy solid at 79% yield.

2.2. Nanoemulsion design and preparation

The ability of PFPE-tyramide nanoemulsions to carry a water-insoluble drug was improved by adding a hydrocarbon oil, neutral medium-chain triglyceride, caprylic-capric acid triglyceride Miglyol 812, an FDA-approved solubilizer. We report a nanoemulsion with a PFPE-tyramide **3** core surrounded by hydrocarbon oil (Miglyol 812), containing a water-insoluble COX-2 inhibitor, celecoxib and NIR dye (CellVue® NIR815, MTTI, Inc.), stabilized in water by surfactants, Fig. 1. The water-insoluble drug celecoxib and lipophilic NIR dye would likely inhabit the same lipophilic (Miglyol 812) region. We propose that the fluorocarbon polymer (PFPE), driven by lipophobicity and hydrophobicity, aggregates at the center of the particle, whereas the phenol moieties interact with the hydrocarbon oil shell. The proposed model is in agreement with other reported PFC nanoemulsions in the presence of organic oils such as safflower oil, where the hydrocarbon (HC) was added to suppress Ostwald ripening of the nanoemulsion. The increased lipophilicity of the PFPE chain upon conjugation to tyramine increases its interaction with HC oil. The Miglyol 812/PFPE-tyramide blend formed during thin film preparation is then further subjected to hydration in presence of surfactants and size reduction by microfluidization. The obtained nanoemulsion would have a monomodal distribution and low PDI only if both the HC and PFC are combined in each droplet into a single system (Fig. 2).

In the preliminary formulation studies, PFPE-tyramide self-assembled into a nanoemulsion with mean droplet size of 190 nm and PDI of 0.26 in the presence of a Pluronic® F68 (BASF) surfactant at a fixed ratio to F68:PFPE-tyramide (0.32:1, w/w). Sonication reduced the diameter to 170 nm (Supplementary Fig. 1). The organic solvents used to make dispersions of PFPE-tyramide and F68 solution used to make nanoemulsions (see Section 4.2.2) had a significant effect on the average particle diameter of the nanoemulsion. PFPE-tyramide, a mostly fluorophilic molecule, does not dissolve in a non-fluorinated solvent, but form a dispersion through self-assembly with lightly turbid appearance. It was found that dissolving F68 in acetone while dispersing PFPE-tyramide in isopropanol yielded smaller particle diameter and PDI than using acetone alone (Supplementary Fig. 2). We argue that using two different solvents achieves more efficient mixing of the nanoemulsion components during thin film formation, ultimately aiding emulsification.

The surfactant addition method had a significant effect on the final droplet size and PDI. Surfactants were, either dissolved in acetone and added prior to creating the thin film, or dissolved in water and added during the hydration step as described in Section 4.2.2. When a primarily hydrophilic surfactant (Pluronic® F68, HLB = 29) was used, droplet size and PDI was similar and independent of surfactant addition method or use of sonication (Supplementary Fig. 3). However, when a more lipophilic surfactant (Pluronic® P105, HLB = 15) was used at the same ratio (0.32:1, w/w), we observed significant differences in size and PDI under different surfactant addition conditions (Supplementary Fig. 4).

2.3. Relationship between formulation methods and achieved ^{19}F concentration

For the imaging reagent to be MR-visible, it must have a sufficient fluorine content, usually more than 10^{11} ^{19}F/cell and 7500 cells/voxel *in vitro* [20–22]. Preparing PFPE-tyramide nanoemulsions with a thin film method followed by hydration with aqueous P105 yielded very small droplets, 110 nm. However, these very small droplets did not contain enough ^{19}F content for imaging, with content of $<10^{10}$ ^{19}F spins/mL (data not shown). The very small droplets made with Pluronic® P105 alone did not incorporate enough PFPE-tyramide into the nanoemulsion to be suitable for imaging (Supplementary Fig. 5). To increase fluorine content while maintaining a low droplet size (<200 nm), an additional surfactant (HLB = 15) was introduced to the thin film, Cremophor® EL (BASF). It was found that as the total amount of surfactant increased, the droplet size decreased, Fig. 2A, and the overall PFPE incorporation increased as measured by ^{19}F NMR, reaching levels necessary for successful *in vivo* imaging, Fig. 2B. Finally, the optimal ratio of total amount of surfactants to PFPE-tyramide was 0.24–0.32:1 (w/w).

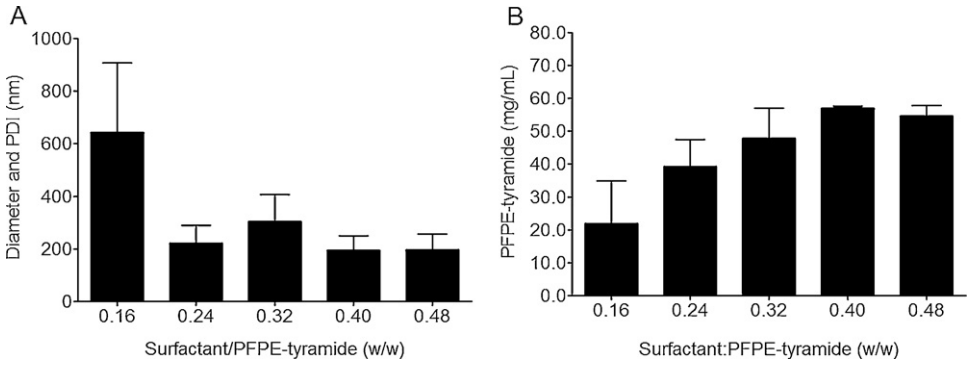

Fig. 2. A) Diameter and PDI of self-assembled PFPE-tyramide nanoemulsions with surfactants Cremophor EL and P105. Nanoemulsions were made with Cremophor EL added during the hydration and P105 in the thin film. (B) PFPE-tyramide concentration of self-assembled PFPE-tyramide nanoemulsions with surfactants ($n = 2$) measured by ^{19}F NMR.

2.4. Incorporation of hydrocarbon oil, NIR dye, and drug

The high hydrophobicity and substantial lipophobicity of the PFPE polymer in PFPE-tyramide conjugate prevents incorporation of lipophilic and water-insoluble drugs. Therefore, several types of natural and synthetic hydrocarbon oils were introduced into the formulation to facilitate incorporation of a lipophilic model drug celecoxib. Our preliminary studies with PFPE-tyramide nanoemulsions incorporated olive oil (Super Refined, Croda) and Capmul (PG-8, Abitec). Olive oil appeared unable to dissolve a sufficient amount of celecoxib (more than 2 mg per 1 g of oil, data not shown) while PFPE-tyramide nanoemulsions with Capmul were unstable (data not shown). Miglyol 812, a mixture of medium chain triglycerides (primarily capric and caprylic acids), could successfully dissolve celecoxib and was used at an equal weight to PFPE-tyramide and formulated into nanoemulsions **A**, **B**, and **C**, Table 1. Nanoemulsion **A** contained PFPE-tyramide, Miglyol 812, Cremophor EL, and P105. Nanoemulsion **B** and **C** contained NIR815 dye, and nanoemulsion **C** carried the model drug celecoxib at 0.2 mg/mL. Fig. 3 shows the droplet size and PDI for pre-emulsions A, B and C prepared by self-assembly. The presence of drug has significant influence on the obtained pre-emulsion droplet size and PDI. Microfluidization reduces the diameter and PDI of all formulations. This data demonstrates the importance of applying high shear processing for forming PFC nanoemulsions, since self-assembly does not produce nanoemulsions with the desired low droplet diameter and PDI. The nanoemulsions were characterized for the droplet size, PDI, zeta potential, and pH, Table 2. Nanoemulsions **A**, **B**, and **C** had average droplet size of 180 nm and PDI < 0.2. Zeta potential was in the region of -70 mV, indicating good stability, and pH was near 5. From drug delivery point of view, droplet size < 200 nm suggests possibly successful passive targeting through the EPR effect in solid tumors [12].

2.5. Stability assessment by dynamic light scattering

Stability of nanoemulsions **A**, **B** and **C** was assessed by measuring droplet size and PDI by Dynamic Light Scattering (DLS) on a Zetasizer Nano (Malvern, UK). Nanoemulsions do not significantly change in size as of 30 days while stored at 4 °C, Fig. 4. Storage at higher temperatures (37 °C) resulted in droplet size increase after 2 weeks on average, while the overall size remained under 300 nm (data not shown). The nanoemulsions were sufficiently stable to pursue biological testing, described in Sections 2.5 and 2.6.

Table 1
Composition of PFPE-tyramide/Miglyol 812 nanoemulsions.

Nanoemulsion	**A**	**B**	**C**
Component	mg/mL	mg/mL	mg/mL
PFPE-tyramide	20	20	20
Miglyol 812	20	20	20
Cremophor EL	5.76	5.76	5.76
P105	3.84	3.84	3.84
Celecoxib	0	0	0.2
Dye	mM	mM	mM
NIR815[a]	0	0.0002	0.0002

[a] CellVue® NIR815, MTTI, Inc.

Table 2
Properties of PFPE-tyramide/Miglyol 812 nanoemulsions.

Nanoemulsion	**A**	**B**	**C**
Diameter (nm)	180.9	182.9	183.2
PDI	0.176	0.182	0.157
Zeta potential (mV)	−73.75	−73.4	−72.6
pH	4.97	5.36	5.23

2.6. In vitro toxicity

Nanoemulsions **B** and **C** were tested for their effect on cell proliferation by MTS colorimetric assay (Promega, Madison, WI) in model immune cells, fetal skin dendritic cells (FSDCs). FSDCs were plated in 96-well plates and exposed to increasing concentrations of nanoemulsion **B**, nanoemulsion **C**, matched concentration of drug in DMSO as in nanoemulsion **C**, and matched volume of DMSO without drug. After 24 h, absorbance was measured at 490 nm on a Perkin Elmer Victor 2 Microplate Reader, Fig. 5. Decreased cell proliferation was observed in nanoemulsions **B** beyond 1 mg/mL, and in nanoemulsion **C** carrying celecoxib doses greater than 0.004 mg/mL. This suggests that celecoxib has likely a different effect on cells once accumulated intracellularly than when celecoxib is delivered in cell culture media. The low solubility of celecoxib in aqueous media can explain this discrepancy. It is likely that much more drug reaches the intracellular compartments when delivered in a nanoemulsion. NIR microscopy suggests the intracytoplasmic location of the celecoxib carrying nanoemulsion **C**, Fig. 6.

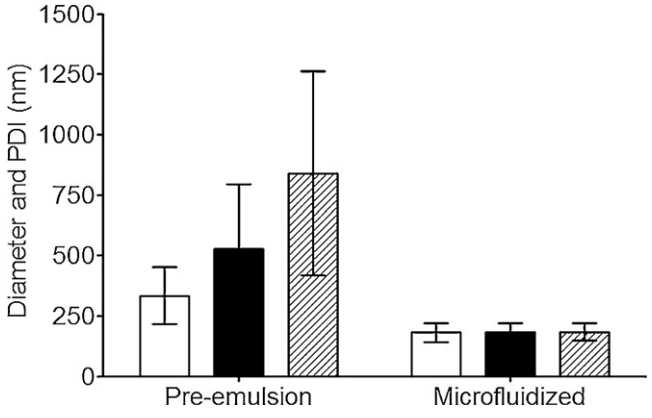

Fig. 3. Diameter of nanoemulsion droplets prepared by self-assembly from a thin film (pre-emulsion, left) and after high shear processing (microfluidized, right) where weight ratio of dry components, PFPE-tyramide/Miglyol 812/surfactants, is 1:1:0.48 (w/w/w). Size after microfluidization for all PFPE-tyramide/Miglyol 812 formulations was around 180 nm, with PDI less than 0.2. Open bars represent the nanoemulsion without drug or dye (**A**). Closed bars represent the nanoemulsion with NIR815 dye (**B**). Striped bars represent the nanoemulsion with drug and NIR815 dye (**C**).

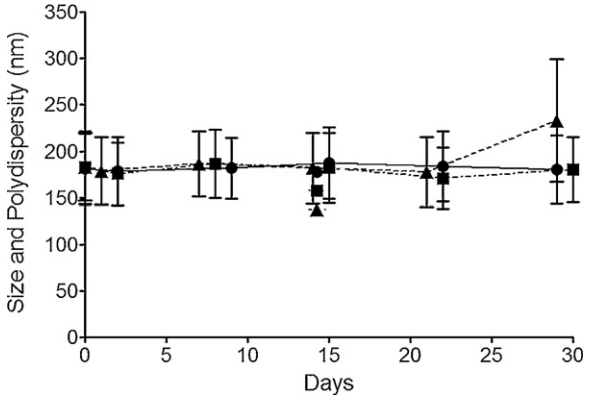

Fig. 4. Average droplet diameter and PDI over time of nanoemulsions **A** (●), **B** (■) and **C** (▲) at stored at 4 °C.

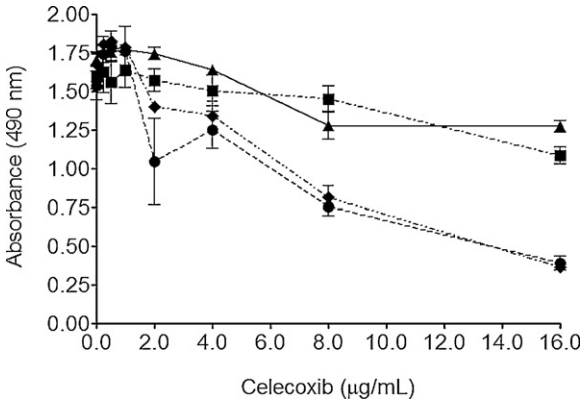

Fig. 5. FSDCs cell proliferation in presence of PFPE-tyramide/Miglyol nanoemulsions. Cells were exposed to increasing doses of nanoemulsions **B** (without celecoxib), **C** (with celecoxib) and celecoxib/DMSO controls over 24 h. Proliferation was assessed with MTS assay. Absorbance was measured at 490 nm on a microplate reader. Diamonds (◆) represent absorbance readings of cells exposed to nanoemulsion **B**, circles (●) represent absorbance readings of cells exposed to nanoemulsion **C**, triangles (▲) represent cells exposed to the same dose of celecoxib in DMSO as in nanoemulsion **C**, and squares (■) represent the matched volumes of the vehicle control (DMSO), without drug.

2.7. In vitro uptake

For potentially theranostic nanoemulsions carrying both imaging agents (PFPE-tyramide, NIR815 dye) and drug, it is critical that the carrier alone does not interfere with the normal cellular function. The drug carrying nanoemulsion (emulsion **C**) must perform in regard to intracellular uptake and cellular viability effects exactly the same as the carrier alone (emulsion **B**). Therefore emulsions **B** and **C** were tested side by side in all cell culture assays. Cellular uptake of both nanoemulsions was visualized by NIR microscopy, Fig. 6, and quantified by ^{19}F NMR spectroscopy of lysed cell pellets, Fig. 7.

No morphological changes were observed and nanoemulsion **B** (Fig. 6B) and **C** (Fig. 6D) apparently accumulated in the cytoplasm after a 3 h exposure. To serve as a true theranostic agent, the nanoemulsion **C** which carries the drug needs to load into the cells at levels needed for optimal future *in vivo* detection. Earlier studies have established needed amount of ^{19}F atoms in each labeled cells necessary for sufficient signal levels in ^{19}F MRI *in vivo*. The nanoemulsion **C** uptake levels $>10^{11}$ ^{19}F/cell are sufficient for necessary for future *in vivo* imaging application and were achieved within a 3 h incubation, Fig. 7A. The cell culture samples for ^{19}F NMR analysis with lysed FSDC pellets exposed to increasing concentrations of nanoemulsion **C** were imaged on an Odyssey

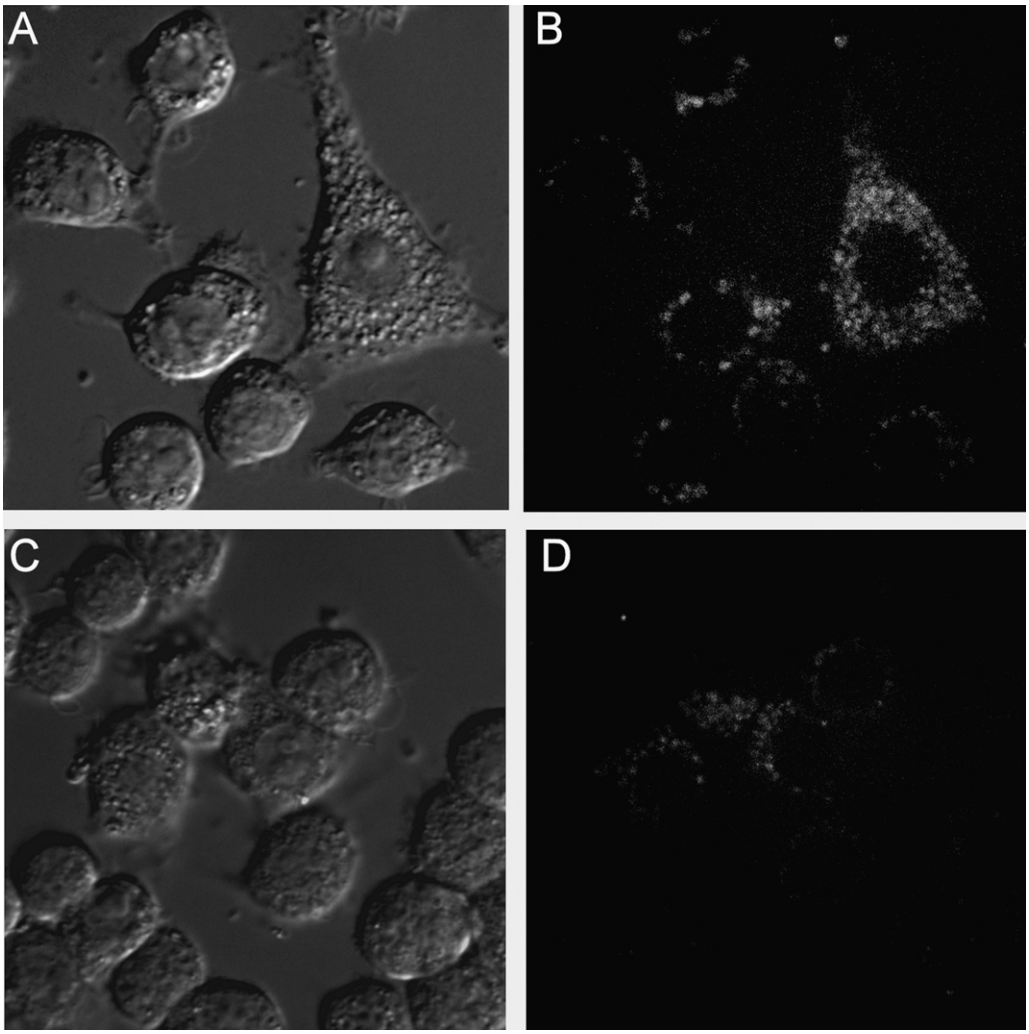

Fig. 6. Microscopy of FSDCs exposed to nanoemulsions **B** and **C**, magnification 60×. A) Differential interference contrast microscopy (DIC) of FSDCs exposed to nanoemulsion **B** (no drug) overnight at 0.5 mg/mL. B) NIR image of FSDCs exposed to nanoemulsion **B**. C) DIC of FSDCs exposed to nanoemulsion **C** (with celecoxib) overnight at 0.5 mg/mL. D) NIR image of FSDCs exposed to nanoemulsion **C**.

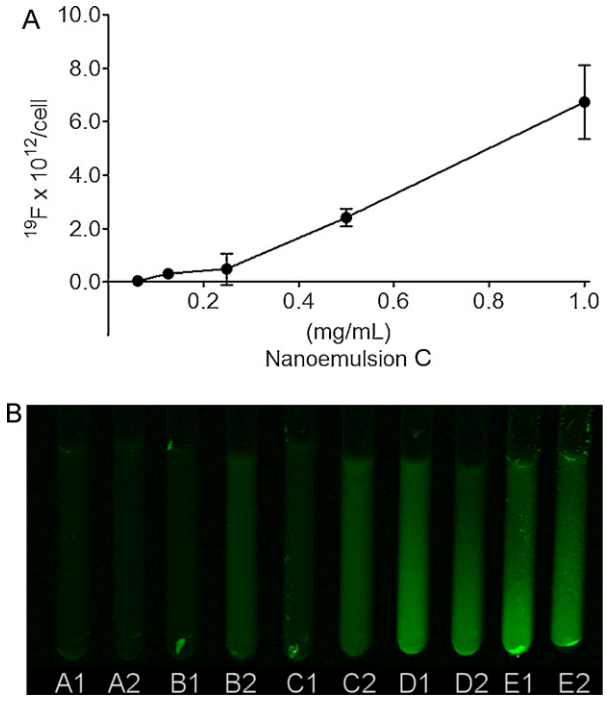

Fig. 7. A) Dose dependent uptake as measured by ^{19}F NMR of nanoemulsion **C** in FSDCs. B) NIR fluorescence imaging (at 800 nm) on Odyssey Infrared Imager (Li-COR) of NMR samples with lysed FSDCs exposed to increasing concentrations of nanoemulsion **C** ($A_{1,2}$ = 0.06, $B_{1,2}$ = 0.13, $C_{1,2}$ = 0.25, $D_{1,2}$ = 0.50, $E_{1,2}$ = 1.00 mg/mL). Images of duplicate samples from a representative experiment are shown.

Infrared Imager (Li-COR) at 800 nm emission detection. The measurements were obtained of the same samples by both techniques to remove any potential bias and provide clear image of the complementarity between two detection techniques, NIR and ^{19}F NMR. Together, these data indicate that theranostic nanoemulsion **C** can be delivered to cells, rendering them detectable by both ^{19}F MR and NIR, carrying a water insoluble drug with an intracellular target, the COX-2 enzyme. Further studies are underway to demonstrate the effectiveness of the drug carrier *in vivo*.

3. Conclusion

PFPE-tyramide was successfully formulated into a drug-carrying nanoemulsion with dual imaging modalities, ^{19}F MR and NIR. The results obtained by DLS, ^{19}F NMR, NIR fluorescence microscopy, and biological studies indicate that the nanoemulsion formulation may be useful for parenteral administration of celecoxib. Further studies are needed to determine whether the PFPE-tyramide nanoemulsion with celecoxib could inhibit tumor growth and if so, the appropriate dosing strategy. Drug-carrying nanoemulsions with imaging agents have the potential to address many of the challenges in water-insoluble drug delivery. In the future, this formulation could carry other water-insoluble anti-cancer or anti-inflammatory drugs while retaining its dual imaging capabilities.

4. Materials and methods

4.1. Materials

PFPE dimethyl ester was purchased from Exfluor Research Corp (Round Rock, TX). Perfluorohexanes were purchased from Synquest (Alachua, FL). Miglyol 812 (caprylic/capric triglycerides) was a kind gift from Sasol (Houston, TX). Pluronic® F68 and P105 were from BASF (Rhineland-Palatinate, Germany). Cremophor EL (ethoxylated castor oil), and trifluoroethanol were from Sigma–Aldrich (St. Louis, MO), and all other reagents and solvents were from Fisher Scientific (Pittsburgh, PA). CellVue NIR815 was a kind gift of Molecular Targeting Technologies Inc. (West Chester, PA). Celecoxib, the model drug for all experiments was purchased from LC Laboratories (Woburn, MA). All reagents were used as received without further purification. Water was deionized.

4.2. Methods

4.2.1. Synthesis of PFPE-tyramide

PFPE-tyramide was synthesized and purified using previously reported protocol [1] with some modifications. PFPE dimethyl ester (10 g, 6 mL, 5.71 mmol, Ave MW = 1750) was added to a 100 mL reaction flask and stirred (1-in. magnetic bar, 350 rpm). 4-(2-Aminoethyl)phenol (Tyramine 97%, Acros, Geel, Belgium) (1.6 g, 11.66 mmol) was suspended in 2,2,2-trifluoroethanol (Acros) (50 mL), vortex mixed (high, 2 min), and added to the reaction flask under an argon atmosphere at R.T. while stirring. The reaction mixture was stirred at R.T. for 51 h and then solvent evaporated on a R-215 rotavapor (Buchi, Flawil, Switzerland) (100 rpm, 30 °C) in a 100 mL round bottom flask. The crude product was dissolved in methanol (20 mL) and loaded into a purification column in a 60 mL coarse Buchner funnel (VWR, Radnor, PA) of silica gel (Geduran, EMD, Darmstadt, Germany) (50 g) packed dry between thin layers of sand. The crude product in methanol was loaded by gravity and the column washed with a perfluorohexanes/hexanes (1:4, v/v) mixture (50 mL); perfluorohexanes/hexanes/methanol (4:16:5, v/v/v) mixture (50 mL); a perfluorohexanes/hexanes/methanol (1:4:5, v/v/v) mixture (50 mL); a perfluorohexanes/hexanes/methanol (1:4:20, v/v/v) mixture (50 mL); and methanol (50 mL), for a total of 5 elutions. Residual solvents from the eluants were removed by vacuum, leaving purified PFPE-tyramide (8.88 g, 4.53 mmol, 79.3%, Ave MW = 1950) as a yellow/tan waxy solid.

4.2.2. PFPE-tyramide nanoemulsion preparation by self-assembly with/without sonication

Nanoemulsions were prepared by combining solutions of PFPE-tyramide in isopropanol and surfactant in acetone. Solutions were added to test tubes and solvents evaporated with air through a Pasteur pipette, resulting in a thin film of PFPE-tyramide and surfactant. The thin film was subsequently hydrated with water or an aqueous surfactant solution while vortex mixing. Sonication, when performed, was done on a Model 500 ultrasonic dismembrator (Fisher Scientific, Pittsburgh, PA) with 3 mm diameter tip at 30% amplitude, with a five second pulse followed by a five second pause for six cycles. Samples were cooled in microcentrifuge tubes on ice for 20 min prior to sonication.

4.2.3. PFPE-tyramide nanoemulsion preparation by microfluidization

Nanoemulsions were prepared by combining solutions of PFPE-tyramide and Miglyol 812 in isopropanol and surfactant in acetone in a round bottom flask. Celecoxib solution in acetone and NIR815 dye stock was added, if applicable. Solutions were stirred for 20 min (350 rpm) at R.T. Solvents were evaporated on a R-215 rotavapor (Buchi, Flawil, Switzerland) at 25 °C, 100 rpm for 1 h. The thin film was subsequently hydrated with water or an aqueous surfactant solution while stirring for 20 min (350 rpm) at R.T. Sonication, when performed, was done in a beaker on a model 500 ultrasonic dismembrator (Fisher Scientific, Pittsburgh, PA) with a 7.5 mm diameter tip at 30% amplitude, with a five second pulse followed by a five second pause for six cycles. The sonicated pre-emulsion was microfluidized in a cooled M-110S microfluidizer (Microfluidics Corp., Newton, MA) for 20 pulses recirculating at 60 psi.

4.2.4. Determination of particle size and PDI by DLS

Nanoemulsion droplet size and PDI were determined by dynamic light scattering (DLS) using a Malvern Zetasizer Nano (Malvern Instruments, Worcestershire, United Kingdom). A HeNe gas laser (λ = 633 nm) with a detector at 173° was used to carry out measurements at 25 °C. Samples were prepared by diluting 5 μL of the sample in 995 μL of deionized water.

4.2.5. Electrophorectic properties (pH and zeta potential)

Zeta potential was measured on a Malvern Zetasizer Nano. 25 μL of each nanoemulsion was diluted in 975 μL of deionized water and measured in a disposable Zeta cell. pH was determined after a two-point calibration (7.00 and 4.01) by Oakton 1100 series pH meter with temperature probe.

4.2.6. ^{19}F NMR characterization

Nuclear magnetic resonance spectrometry was used to measure the ^{19}F concentration of nanoemulsions and cells. ^{19}F NMR chemical shifts were reported as ppm using a trifluoroacetic acid (TFA) reference added at 0.1% (v/v) or 0.01% (v/v) to the nanoemulsion sample or cells in media, with chemical shift set at −76.0 ppm. PFPE-tyramide nanoemulsions show a peak at −91.1 ppm and cells containing PFPE-tyramide show a peak at −91.4 ppm. The resulting spectral peaks were integrated and the resulting areas can be used to calculate the mean ^{19}F concentration per volume nanoemulsion or per cell.

4.2.7. Cell culture

Fetal skin dendritic cells (FSDCs) were cultured at 37 °C under a 5% CO_2 humidified atmosphere in Dubelco's modified Eagle medium (DMEM, Mediatech, Inc., Manassas, VA) supplemented with 10% HyClone Fetal Bovine Serum (FBS, ThermoScientific, USA), 1% penicillin/streptomycin (1:1) solution, 1% Hank's Balanced Salt Solution (HBSS), 4.5 g/mL D(+) glucose, and 1% L-glutamine.

4.2.8. NIR fluorescence microscopy

FSDCs are plated in glass bottom confocal microscopy dishes and let attach overnight in complete media (10% FBS, DMEM with 4.5 g/mL glucose) and incubated at 37 °C and 5% CO_2. Adherent cells are washed with warm media (37 °C) and exposed to nanoemulsion **C** at 0.5 mg/mL for 3 h. Emulsion containing media is removed by vacuum aspiration, cells washed twice with phosphate buffer and imaged on a fluorescent microscope (Andor Revolution XD Spinning Disk Confocal microscope) where NIR dye is detected at 780 nm, Fig. 6.

4.2.9. In vitro toxicity

CellTiter 96 AQueous Non-Radioactive Cell Proliferation Assay (Promega, Madison, WI) was used to assess cytotoxicity of nanoemulsions **B** and **C** after a 24 h exposure time at concentration range 0 to 4 mg/mL in a 96-well plate (triplicate samples). The cells were then exposed to MTS for 2 h. Dehydrogenase enzymes active in living cells reduced MTS to a formazan product that was quantified by a UV–Vis plate reader (Li-COR Odyssey® NIR imager, Lincoln, NE) set to measure absorbance at 490 nm. The number of living cells was proportional to the absorbance measurement. Cells exposed to nanoemulsions were compared to untreated cells.

4.2.10. In vitro uptake measurements by ^{19}F NMR

Uptake of nanoemulsion **C** was demonstrated in FSDCs. Cells are plated in 6-well plates, 1–2 × 10^6/well, and allowed to attach overnight. Immediately before cell labeling, emulsion was diluted in Dubelco's modified Eagle medium (DMEM) supplemented with 10% (v/v) fetal bovine serum (FBS). Nanoemulsion containing medium was added to cells at 2 mL/well. After 3 h incubation at 37 °C, medium was removed, and cells were washed two times with phosphate buffered saline (PBS), detached by trypsinization, washed, and resuspended in 1 mL of complete medium for cell counting and Trypan Blue exclusion assay (Sigma Aldrich). The cells were pelleted and resuspended in 0.2 mL of 1% (v/v) deionized water, incubated at R.T. for 20 min, mixed with 0.02% (v/v) TFA solution in water (set at 76.0 ppm) and used for ^{19}F NMR measurements The PFPE-tyramide containing cells show a major peak at −91.4 ppm. The integrated areas under these two peaks can be used to calculate the mean ^{19}F/cell, ranging from 10^{11} to 10^{12}, as reported previously [21,22].

4.2.11. NIR spectroscopy

^{19}F NMR samples, prepared above, are used to measure NIR fluorescence. Lysed cell pellets in 0.4 mL of aqueous solution were transferred to 5 mm NMR tubes. The tubes were placed horizontally on the glass sample holder on Odyssey Imager (Li-COR Biosciences, Lincoln, NE) and fluorescence signal collected at 800 nm emission wavelength.

Acknowledgements

We would like to thank Virgil Simplaceanu of the Pittsburgh NMR Center for help with ^{19}F NMR and Michael J. Patrick for his assistance with fluorescent microscopy. We also thank Sravan K. Patel, Dr. Ira S. Buckner, and Michael J. Patrick for their assistance, manuscript review and helpful discussions. This work was supported by NIH 1R41EB009618-01A1, the Commonwealth Universal Research Enhancement Program of the Pennsylvania Department of Health, and the Duquesne University Faculty Development Fund.

Appendix A. Supplementary data

Supplementary data associated with this article can be found, in the online version, at doi:10.1016/j.jfluchem.2012.02.004.

References

[1] S.M. Janib, A.S. Moses, J.A. MacKay, Adv. Drug Deliv. Rev. 62 (2010) 1052–1063.
[2] A. Gianella, P.A. Jarzyna, V. Mani, S. Ramachandran, C. Calcagno, J. Tang, B. Kann, W.J.R. Dijk, V.L. Thijssen, A.W. Griffioen, G. Storm, Z.A. Fayad, W.J.M Mulder, ACS Nano 5 (2011) 4422–4433.
[3] G. Chen, L. Wang, Curr. Pharm. Des. 17 (2011) 2331–2351.
[4] J.M. Janjic, E.T. Ahrens, WIREs Nanomed. Nanobiotechnol. 1 (2009) 492–501.
[5] T.K. Hitchens, Q. Ye, D.F. Eytan, J.M. Janjic, E.T. Ahrens, C. Ho, Magn. Reson. Med. 65 (4) (2011) 1145–1154.
[6] E.T. Ahrens, W. Young, H. Xu, L.K. Pusateri, Biotechniques 50 (4) (2011) 229–234.
[7] N.R. Soman, G.M. Lanza, J.M. Heuser, P.H. Schlesinger, S.A. Wickline, Nano Lett. 8 (4) (2008) 1131–1136.
[8] T.J. Wooster, M. Golding, P. Sanguansri, Langmuir 24 (2008) 12758–12765.
[9] J.V. Frangioni, Curr. Opin. Chem. Biol. 7 (2003) 626–634.
[10] Y.T. Lim, Y.-W. Noh, J.-N. Kwon, B.H. Chung, Chem. Commun. 45 (2009) 6952–6954.
[11] P. Mohan, N. Rapoport, Mol. Pharm. 7 (6) (2010) 1959–1973.
[12] H. Maeda, Adv. Enzyme Regul. 41 (2001) 189–207.
[13] V. Torchillin, Adv. Drug Deliv. Rev. 63 (3) (2010) 131–135.
[14] J.B. Cannon, Y. Shi, P. Gupta, in: R. Liu (Ed.), Water-Insoluble Drug Formulation, second ed., CRC Press, Boca Raton, 2008, pp. 195–254.
[15] F. Pagès, J. Galon, M.-C. Dieu-Nosjean, E. Tartour, C. Sautès-Fridman, W.-H. Fridman, Oncogene 29 (2010) 1093–1102.
[16] J.R. Mann, M.G. Backlund, R.N. DuBois, Nat. Clin. Pract. Oncol. 2 (2005) 202–210.
[17] C. Porta, P. Larghi, M. Rimoldi, M.G. Totaro, P. Allavena, A. Mantovani, A. Sica, Immunobiology 214 (2009) 761–777.
[18] Y.S. Zhao, S. Zhu, X.W. Li, F. Wang, F.L. Hu, D.D. Li, W.C. Zhang, X. Li, Breast Cancer Res. Treat. 117 (2009) 141–150.
[19] J.G. Riess, Tetrahedron 58 (20) (2002) 4113–4131.
[20] M.P. Krafft, J.G. Riess, Chem. Rev. 109 (2009) 1714–1792.
[21] J.M. Janjic, M. Srinivas, D.K.K. Kadayakkara, E.T. Ahrens, J. Am. Chem. Soc. 130 (9) (2008) 2832–2841.
[22] M. Srinivas, P.A. Morel, L.A. Ernst, D.H. Laidlaw, E.T. Ahrens, Magn. Reson. Med. 58 (4) (2007) 725–734.